EOS Trans. AGU, 79, 613, December 1998.

Maps Could Provide Space Weather Forecasts for the Inner Magnetosphere

Geoffrey Reeves, Reiner Friedel, and Robin Hayes

Introduction

If you are like many people you scan the newspaper, television, or internet every morning and check out the latest weather map and forecast to see how it may affect what you plan to do that day. If you depend on satellites to do your business and you want to know how the "weather" in space might affect those satellites you aren't so lucky – at least not yet.

"Space Weather" is a relatively new term in space physics. Broadly, it refers to the conditions in space that may affect human activities. Those conditions are changing all the time. Differing types and intensities of solar activity produce different conditions in the solar wind which in turn impacts the conditions in the magnetosphere, ionosphere, and upper atmosphere. Adverse space weather conditions include increased ionospheric scintillation which disrupts communications and navigation signals, electrical charging of spacecraft surfaces which can produce arcing, and radiation damage from energetic protons and electrons which can damage spacecraft components. Space weather has been implicated as cause or contributing factor in a number of satellite failures (such as Anik, Telstar 401, and Galaxy IV) that have resulted in sudden blackouts of TV, radio, and communications systems. Space weather is also a significant concern for human activities in space, particularly extra-vehicular activities where astronauts can be exposed to increased radiation doses. There is a clear need for better ways to specify the conditions in space and to create tools that are useful to the users and operators of space systems as well as to space physics researchers.

This article describes the development of "weather maps" for the radiation environment in the inner magnetosphere. In analogy with traditional weather maps the objective is to take data from an array of monitors and to synthesize those data into a picture of the space environment (Figure 1). Obviously there are some differences. Instead of cloud cover or barometric pressure, space weather maps need to display particle fluxes and plasma temperatures and densities. In place of cold fronts we need to represent the locations of boundaries such as the magnetopause or plasmasphere.

There are a number of possible approaches to producing space weather maps, each with particular strengths and weaknesses. One class of models, often called theoretical or physics-based, includes global magneto-hydrodynamic (MHD) models, single-particle drift models, and particle diffusion codes that strictly adhere to a given set of equations but make rather limited use of in situ measurements. At the other extreme are empirical or data-based models that are based primarily on a set of measurements rather than a set of equations. Typically empirical models bin data according to location and/or activity level (e.g. Kp, Dst, or Solar Cycle) to produce an average representation of a particular population. While these models are extensively used for instrument and

spacecraft design they are not dynamic and do not represent current or even recent conditions.

We describe here a new approach to data-based modeling that is explicitly designed to represent the temporal as well as spatial variations in the inner magnetosphere. We have applied the technique to two populations that are of practical concern: (1) the injection of energetic electrons during substorms which contributes to spacecraft surface charging and (2) the enhancement of the radiation belts during geomagnetic storms which contributes to deep dielectric charging in internal spacecraft components.

A Real-Time Substorm Injection Model

Magnetospheric substorms are the fundamental process through which energy and magnetic flux that get coupled to the magnetosphere from the solar wind are released and redistributed. Part of that process is the injection of energetic (10's-100's keV) electrons and protons into the inner magnetosphere. Substorm injections are most commonly observed at geosynchronous orbit, at 6.6 Earth Radii (R_E), both because most substorms produce injections in that region and because there are many satellites that operate there.

Being in space, satellites are, of course, not grounded. Electric charge can build up on the surface of the spacecraft if a different number of electrons and protons strike the surface. One part of a satellite can charge more than another part which can eventually lead to electrostatic discharges which in turn can damage components such as arrays of solar cells. The injection of hot (energetic) electrons during substorms increases spacecraft charging. Most surface charging related spacecraft "anomalies" occur in the midnight to dawn sections of the magnetosphere where the hot electrons are injected.

To support the US Air Force Space Weather program, Los Alamos National Laboratory has monitored substorm injections at geosynchronous orbit continuously since 1976 [Reeves et al., 1996]. Typically three satellites provide data simultaneously and in near real time. However, geosynchronous orbit is over a quarter-million kilometers long, hundreds of satellites operate there, and only a few of them have energetic particle detectors.

Therefore we must determine the fluxes everywhere along the orbit based on a few measurements. We do this using the single-particle drift equations. An electron (or ion) in the Earth's magnetic field will drift azimuthally due to the gradient and curvature of the field. Electrons drift east and ions drift west. Therefore, knowing the drift velocity, we can project our measurements forward and backward in time to specify the fluxes at other locations. With multiple satellites we can determine the electron fluxes between any pair by projecting the western satellite's measurements east and forward in time and by projecting the eastern satellite's measurements west and backward in time. At the point where we wish to know the fluxes we take a weighted average of the time-shifted fluxes. The weighting is based on how close the point is, in azimuth, to each of the satellites.

Figure 2 illustrates the result. The measurements from satellite 1982-019 at 70° east longitude are plotted in blue while the measurements from satellite 1977-007 at 70° west are plotted in magenta. The model fluxes at each 10° step in longitude between the satellites are also plotted. By design there is a smooth transition from one satellite to the next.

Although this figure shows a time series for 24 hours the fluxes are specified for each longitude and each local time based on current measurements so the data can be displayed in a variety of ways. This data-based technique does not predict when a substorm injection will occur but once an injection has been detected it does predict when the injected electrons will reach a particular satellite and how intense they may be. In future work this technique could be combined with other predictive techniques such as neural networks to further improve the forecasting capabilities. However, even without predictive capabilities, the fact that this model works with a continuous source of real-time data makes it practical for operational use.

Radiation Belt Weather Maps

The Earth's radiation belts also contain a population of higher-energy, relativistic electrons that are of particular concern for spacecraft operations. Electrons with energies greater than a few MeV can penetrate the skin of a spacecraft and embed themselves in materials within the spacecraft. In insulators, such as those used in cables and electronics, the embedded charge leaks off slowly and charge can build up within the material to a point where it discharges causing spurious electrical signals and/or physical damage. This process, known as deep dielectric charging [Vampola, 1987], can cause serious spacecraft anomalies including the complete failure of some satellites [e.g. Baker et al., 1994]. Two recent relativistic electron events that have drawn considerable public as well as scientific attention occurred in January 1997 [e.g. Reeves et al., 1998a,b] and May 1998 [e.g. Baker et al., 1998].

One of the challenges for space research as well as for space weather application is to produce a global composite picture of the radiation belts, from a wide variety of sources, during these highly disturbed conditions. Relativistic electron events are particularly well-suited for making global maps that extend the technique described above into two dimensions – radius and azimuth. Relativistic electron fluxes typically change on a time scale of hours so the two-dimensional distribution can be determined by a relatively small number of satellites. The relativistic electron belts also have a peak intensity well inside geosynchronous orbit varying between about 3.5 and 5 R_E.

Fortunately, more and more satellites are being instrumented with detectors that can measure relativistic electrons. During the January 1997 storm there was data from eleven satellites in a variety of orbits (Table 1). These included the GOES and LANL measurements at geosynchronous orbit, 3 Global Positioning System (GPS) satellites, a highly-elliptical orbit (HEO) satellite, and two NASA satellites – SAMPEX at low altitude and POLAR at high altitude. Reeves et al., [1998b] presented a detailed

analysis of the MeV electron environment during the January 1997 storm. Here we use those same data to demonstrate the global data synthesis model.

As with the substorm injection synthesis the radiation belt synthesis begins with geosynchronous orbit where the density of satellites is highest. In this case the interpolation scheme is simpler than that used for substorms. GOES data is only available at 5 min resolution, which is comparable to the drift period for a 2 MeV electron. Therefore there is no point in time-shifting the data and the weighted average becomes a simple linear interpolation in azimuth. If the Earth's magnetic field were azimuthally symmetric (e.g. a dipole) we would expect no local time asymmetry in the electron fluxes. Therefore the observed differences in electron fluxes reflect the distortions of the magnetic field.

After interpolation we have a complete specification of the >2 MeV electron fluxes at one radius, L=6.6. The next task is to incorporate information about other radial distances. Figure 3 illustrates the steps in this process. First the fluxes are projected into the equatorial plane along magnetic field lines (Figure 3a). Here we found that a 3-hour time window provides a good compromise between time resolution and spatial coverage. Next the data are binned into radius (0.5 R_E) and local time (1 hour MLT) (Figure 3b). Finally a linear interpolation in local time is done between bins at a given radius to complete the global synthesis (Figure 3b). No smoothing or interpolation in radius is done because particles tend to drift in roughly circular orbits and because radial diffusion is relatively slow. Because of the different energies and calibration of the various detectors normalization of the data sets to one another is necessary. The details of the calculation are discussed by Friedel et al., [1998].

A complete two-dimensional map is produced for each 3-hour time window (Figure 4). While some of the details of the flux variations are naturally lost, the synthesis rather strictly adheres to the measurements at the points where measurements were available (e.g. Figure 3a). In addition the synthesis provides a much more intuitive picture of changes in the radiation belts than one gets from looking at separate plots of the data from each satellite.

Figure 4 shows a comparison between line plots of the geosynchronous fluxes and the synthesis maps. Line plots of the other satellites' data are more difficult to interpret because their orbits take them through different drift shells at different times and at different magnetic latitudes.

Prior to the beginning of the event on January 10 the >2 MeV electron fluxes were relatively low and most satellites measured fluxes at or near background levels (Figure 4a). A rapid enhancement of fluxes was caused by the passage of a coronal mass ejection in the solar wind [e.g. Reeves et al., 1998a]. Fluxes between 4 and 7 R_E increased by more than two orders of magnitude, however, the increase was not uniform throughout the magnetosphere Synthesis 4b covers 2100 to 2400 UT on January 10. At geosynchronous orbit, as seen in both the line plots and 2D maps, the highest fluxes were measured by GOES-9 located near local noon whereas at 5 R_E the fluxes were relatively symmetric except for a region of low fluxes near dawn. Several hours later (Figure 4c: 0300-0600 UT on January

11) the fluxes at geosynchronous orbit had decreased significantly and become more uniform in local time . The fluxes at 4-5 R_E, on the other hand, remained relatively high but developed a marked asymmetry, peaking in the midnight to dawn region Figure 4d shows the continued decrease in fluxes and a shift of the 4-5 R_E peak fluxes toward noon. This synthesis also clearly shows the slot region between the inner and outer electron belts, near $3R_E$. From January 12 to January 15 the geosynchronous fluxes slowly built up again perhaps as a result of outward radial diffusion from the more stably trapped source at 4 R_E [Reeves et al., 1998b]. While a quiet-level diurnal variation is still apparent in the geosynchronous line plots this factor of 2-3 variation is too weak to be observed in Figure 4e where radial gradients dominate the color scale.

Conclusions

We believe that it is now possible to produce space weather maps of the energetic particle fluxes in the inner magnetosphere on a regular and continuous basis. The maps that are produced by the technique described here are visually compelling and informative. They are simple enough to be interpreted by non-experts yet contain enough technical information to serve as useful summary plots for scientific investigations.

In contrast to more theoretical techniques the data synthesis does not produce a consistent electric or magnetic field model to go along with the particle flux models. On the other hand, knowing that energetic electrons follow magnetic drift trajectories the maps themselves could be used as a means to specify some of the global magnetic field structure. The empirical, data-based synthesis maps may, in the future, be fruitfully combined with other theoretical, physics-based models such as MHD or particle diffusion codes to their mutual benefit.

The development of “space weather maps”, by various means, is an important step in making scientific measurements widely available and easily interpretable. In terrestrial weather forecasting the National Weather Service provides a valuable service to a wide variety of activities from citrus growing, to summer vacations, to military planning. The information is expensive to acquire yet freely available because it has a recognized pay-off in national economic growth and in reduction of risk. Space weather forecasting, by contrast, is in it’s infancy. But, as society moves into space and becomes more reliant on new space systems, such as GPS, Irridium, or Icos, the value of space weather forecasting will only increase. While the world may not yet be ready for “The Space Weather Channel”, some scientists and policy-makers are already preparing for that day. This effort represents one step toward that goal.

References

Baker, D. N., J. H. Allen, S. G. Kanekal, and G. D. Reeves, Space Environmental Conditions During April and May 1998: An Indicator for the Upcoming Solar Maximum, *EOS Trans. AGU, submitted*, 1998.

Baker, D. N., S. Kanekal, J. B. Blake, B. Klecker, and G. Rostoker, Satellite anomalies linked to electron increase in the magnetosphere, *EOS Trans. AGU, 75*, 410, 1994.

Friedel, R. H. W., G. D. Reeves, R. D. Belian, T. E. Cayton, C. Mouikis, A. Korth, J. B. Blake, J. F. Fennell, R. S. Selesnick, D. N. Baker, T. Onsager, and S. Kanekal, A multi-spacecraft synthesis of relativistic electrons in the inner magnetosphere using LANL, GOES, GPS, SAMPEX, HEO, and POLAR, *Radiation Meas. J., submitted*, 1998.

Reeves, G. D., R. H. W. Friedel, M. G. Henderson, R. D. Belian, M. M. Meier, D. N. Baker, T. Onsager, and H. J. Singer, The Relativistic

Electron Response at Geosynchronous Orbit During the January 1997 Magnetic Storm, *J. Geophys. Res., 103*, 17,559, 1998*a*.

Reeves, G. D., D. N. Baker, R. D. Belian, J. B. Blake, T. E. Cayton, J. F. Fennell, R. H. W. Friedel, M. G. Henderson, S. Kanekal, X. Li, M. M. Meier, T. Onsager, R. S. Selesnick, and H. E. Spence, The Global Response of Relativistic Radiation Belt Electrons to the January 1997 Magnetic Cloud, *Geophys. Res. Lett., submitted*, 1998*b*.

Reeves, G. D., R. D. Belian, T. C. Cayton, R. A. Christensen, M. G. Henderson, and P. S. McLachlan, Los Alamos Space Weather Data Products: On Line and On Time, *in Substorms 3*, ESA SP-339, 689-694, 1996.

Vampola, A. L., The aerospace environment at high altitudes and its implications for spacecraft charging and communications, *J. Electrostat., 20*, 21, 1987.

Acknowledgments. We gratefully acknowledge the US Department of Energy, the National Aeronautics and Space Administration, the National Science Foundation, and Hughes Space and Communications Company for support of this work. We are also grateful to D. N. Baker, R. D. Belian, J. B. Blake, T. E. Cayton, J. F. Fennell, M. G. Henderson, S. Kanekal, X. Li, M. M. Meier, T. Onsager, R. S. Selesnick, and H. E. Spence for their valuable inputs.

G. D. Reeves, Los Alamos National Laboratory, Los Alamos, NM 87545.

(e-mail: reeves@lanl.gov;)

Figure Captions

Figure 1. A familiar surface weather map from The Weather Channel and a fictional version of what a comparable "Space Weather" map might look like.

Figure 2. A one-dimensional data synthesis of substorm injections at geosynchronous orbit. Electron fluxes measured at two satellites at ±70° longitude are time shifted according to the electron drift velocities then averaged to get the predicted flux at any other point in longitude of local time.

Figure 3. An illustration of the construction of a global two-dimensional radiation belt map. (A) Data taken in a 3-hour time window are projected into the equatorial plane along magnetic field lines. (B) Data are averaged into radial and local time bins. (C) The map is filled in by linear interpolation in local time at each fixed radius to complete the synthesis.

Figure 4. A comparison between the two-dimensional data synthesis maps and geosynchronous line plots for the January 1997 geomagnetic storm. At geosynchronous orbit the two plots show the same data but the 2D plots include data from the other six satellites and are more visually intuitive. All synthesis plots use the same color scale. White areas indicate no data coverage for that interval.

Table 1

Satellite	GOES	LANL	GPS	POLAR	SAMPEX	HEO
Number	2	3	3	1	1	1
Energies	>2 MeV	>1.8 MeV	1.6-3.2 MeV	1.9-10 MeV	>1 MeV	>1.5 MeV
Orbit	6.6 R_E, 24 hr circular	6.6 R_E, 24 hr circular	4.2 R_E, 45°, 12 hr circular	2x9 R_E, 18 hr elliptical	600 km, 83°, 90 min circular	1.1x7 R_E, 12 hr elliptical
Data Source	NOAA/SEC	DoE/LANL	DoE/LANL	NASA	NASA	Aerospace Corp.

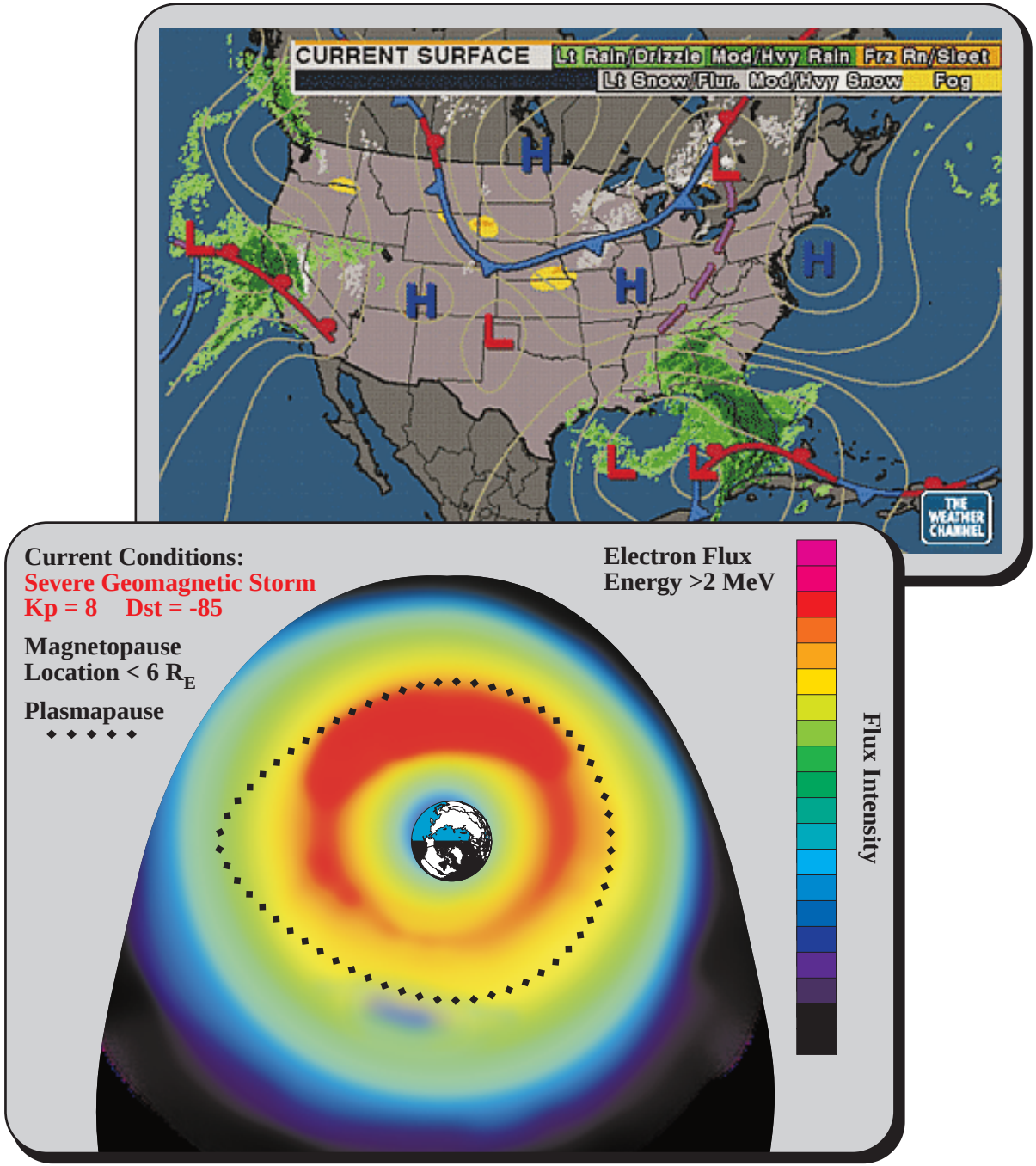

Reeves et al
EOS Trans 1998
Figure 1

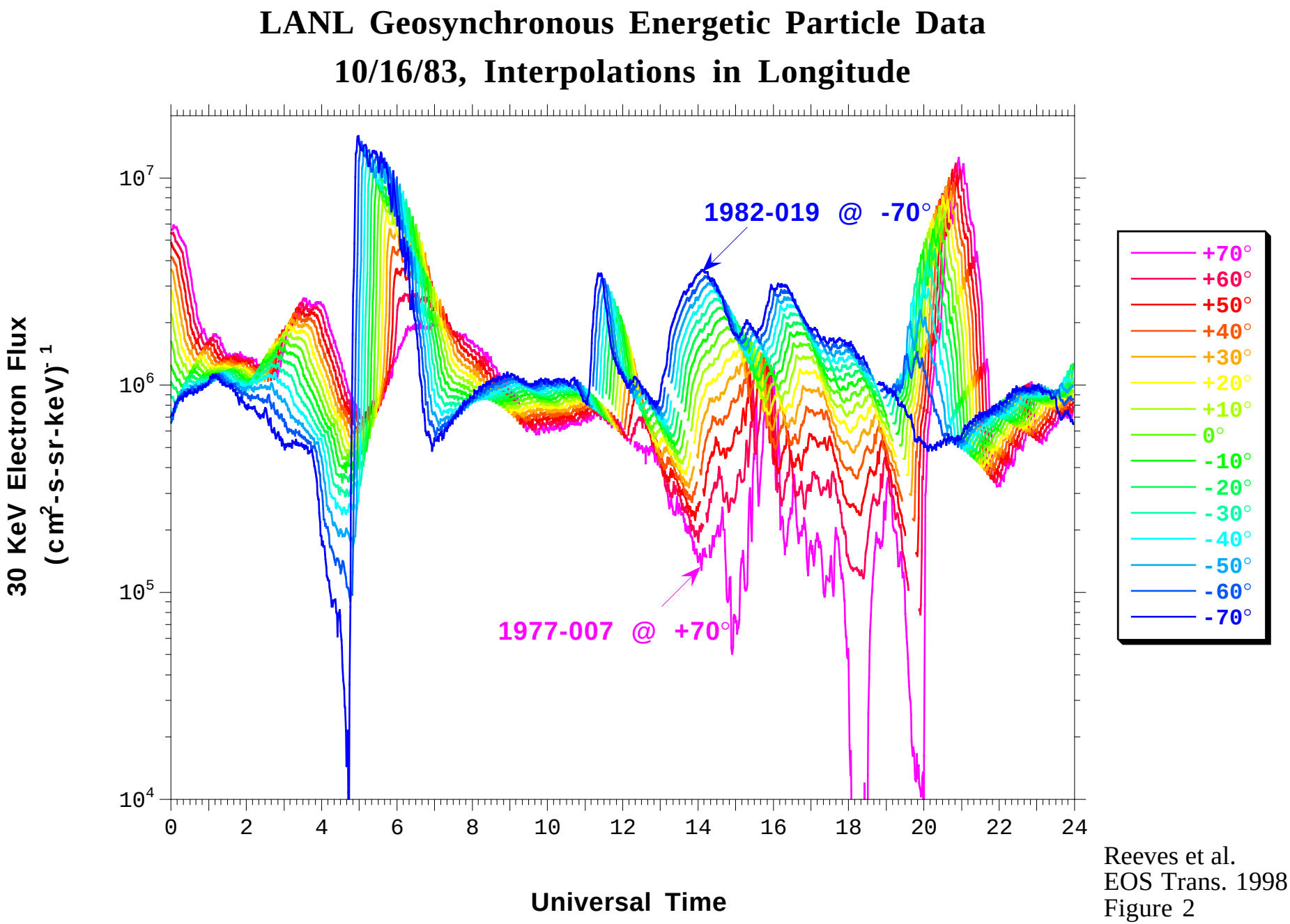

Reeves et al.
EOS Trans. 1998
Figure 2

A

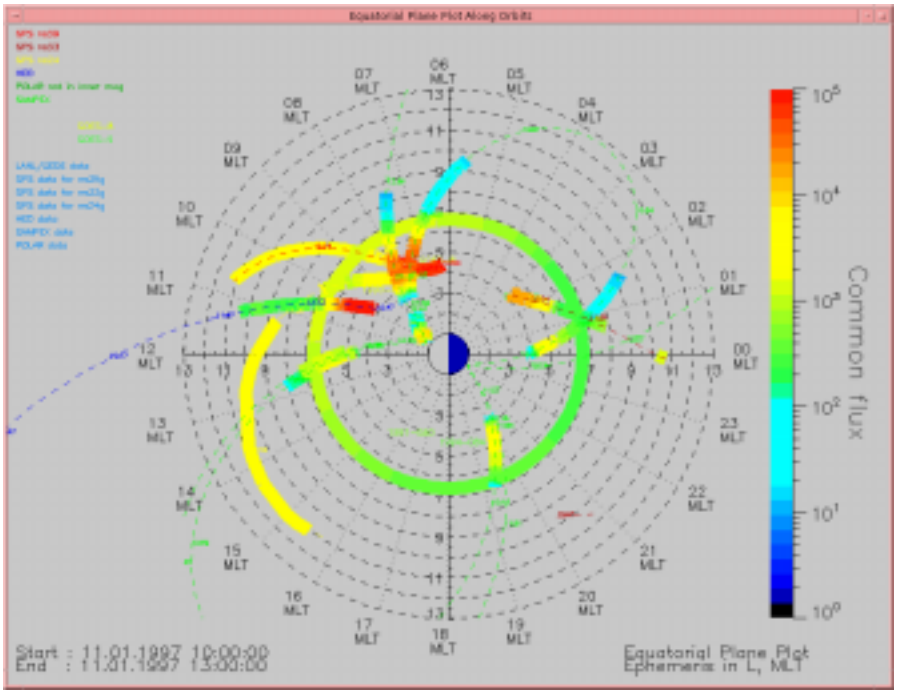

B

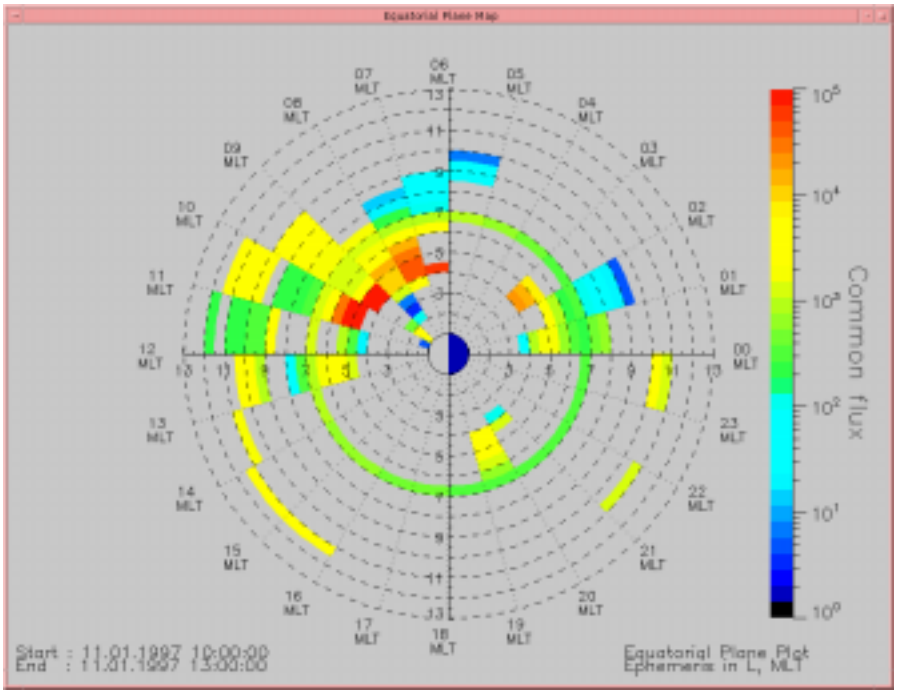

C

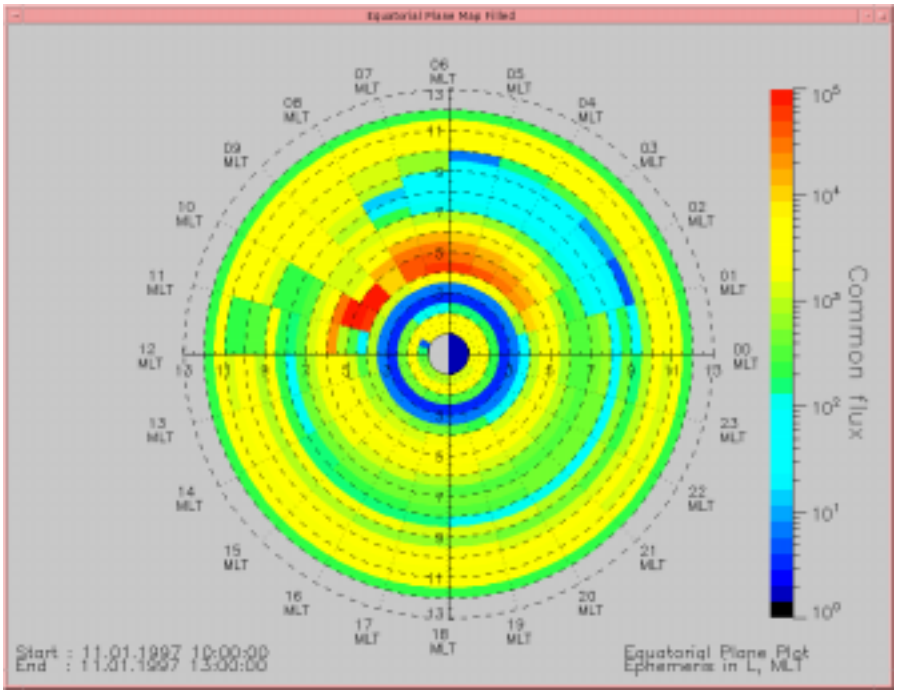

Reeves et al
EOS Trans 1998
Figure 3

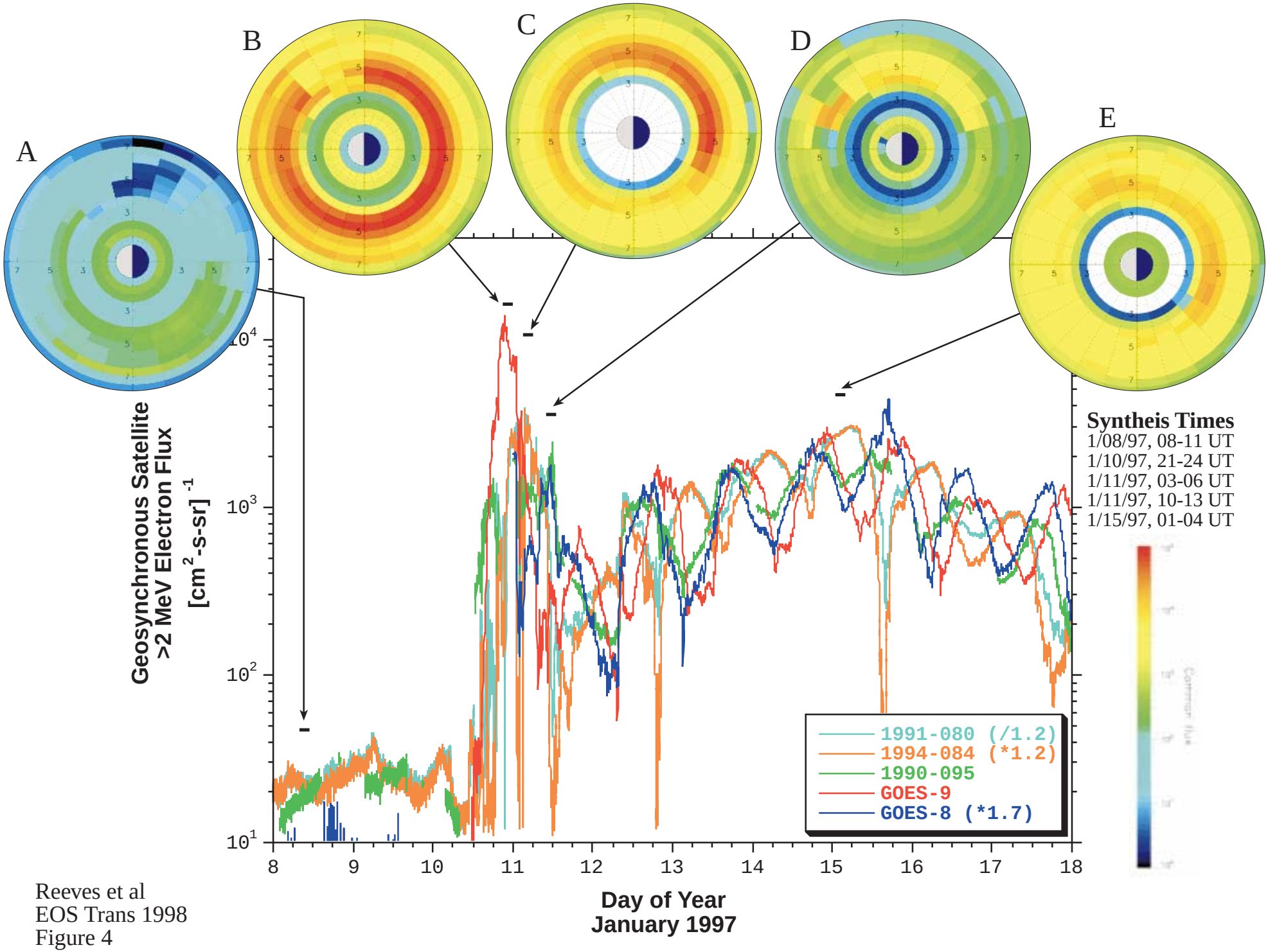

Reeves et al
EOS Trans 1998
Figure 4